RAPID COMMUNICATIONS

PHYSICAL REVIEW B VOLUME 48, NUMBER 17 1 NOVEMBER 1993-I

Effect of transport currents on the critical state of $YBa_2Cu_3O_{7-\delta}$ thin films

M. Darwin, J. Deak, L. Hou, and M. McElfresh
Physics Department, Purdue University, West Lafayette, Indiana 47907

E. Zeldov
Physics Department, Weizmann Institute of Science, Rehovot, 76100, Israel

John R. Clem
Ames Laboratory and Department of Physics and Astronomy, Iowa State University, Ames, Iowa 50011

M. Indenbom*
Max-Planck-Institut für Metallforschung, Institut für Physik, Heisenbergstrasse 1, D-7000 Stuttgart 80, Germany
(Received 7 June 1993)

After preparation of the remanent critical state, the normal component of the local time-dependent magnet field B_z near the surface of a $YBa_2Cu_3O_{7-\delta}$ thin film was measured before, during, and after the application of a transport current. The results are shown to be consistent with new calculations of B_z for the thin film geometry. The calculated behavior in a thin film is shown to be substantially different from that of the Bean critical state in a long slab in a parallel field. In slab geometry, starting from the remanent critical state, $|J(x)|$ is always equal to J_c, whereas in thin films a continuous distribution of current densities $J(x)$ is found. This feature results in a unique distribution of the magnetic field B_z and unusual magnetic relaxation behavior in the presence of a transport current.

The critical-state model[1,2] is commonly used to describe the quasistatic penetration of magnetic flux via quantized vortices into type-II superconductors. Its application is often illustrated by considering a slab in a parallel applied magnetic field. For example, in an increasing applied field above the lower critical field H_{c1}, this model states that the internal magnetic induction $\mathbf{B}$ near the surface obeys $|dB_z/dx|=4\pi J_c/c$, where J_c is the critical-current density. At a sufficiently high applied field, this critical gradient penetrates to the center of the sample, and the magnitude of the induced current density J is equal to J_c throughout the sample. When the applied magnetic field is reduced, the current density induced near the surface reverses direction, but the magnitude of J remains everywhere equal to J_c. This model has been used to analyze numerous magnetization experiments by applying fields parallel to slabs or cylinders, where the behavior is similar.[3-5]

Much less is known, however, about the details of penetration of magnetic flux into a thin-film sample when a magnetic field is applied perpendicular to the film surface. This case is complicated by demagnetization effects and by the fact that in the expression $|\mathbf{J}|=J_c$, where $4\pi\mathbf{J}/c=\nabla\times\mathbf{B}$, both the gradient and the curvature of $\mathbf{B}$ are important. In fact, for a thin film the dominant contribution to the current density arises from the curvature of $\mathbf{B}$.[6] Moreover, in contrast to the above behavior in a slab where the induced current initially flows only near the surface, the surface of the film is exposed to magnetic field components that bend around the film, thereby inducing currents everywhere in the film, not just at the edge. The distribution of induced currents in a superconducting strip in response to small applied magnetic fields or transport currents can be calculated using conformal mapping methods, as described in Refs. 7–9.

In this paper we use a small Hall sensor, placed just above the surface of a $YBa_2Cu_3O_{7-\delta}$ (YBCO) thin film to study the evolution of the local magnetic field as a transport current is applied to a sample initially in the remanent (trapped-flux) critical state. To understand the results, we develop a theoretical method for analytically calculating the hysteretic field and current distributions in a superconducting film whose thickness d is on the order of the penetration depth λ. We apply this method to calculate the field and current distribution as a function of the applied transport current. We find that, in striking contrast to the case of slab geometry, there is a region of the sample for which $0<|\mathbf{J}|<J_c$ and vortices are immobile, while, in common with the slab geometry, $|\mathbf{J}|=J_c$ along the edges of film, where vortices move into or out of the sample. An effect of the corresponding magnetic field distribution is the unusual magnetic relaxation behavior we observe in the presence of a transport current.

An epitaxial YBCO thin film, with the c axis perpendicular to the film plane, was prepared by pulsed laser deposition on a heated (001) $LaAlO_3$ substrate. The film thickness was 3000 ± 500 Å. The superconducting transition temperature (T_c) was 91 K, and the transition width ΔT_c was about 2 K as measured by ac susceptibility at 2.5 MHz.

The normal component of the local magnetic induction (B_z) was measured using a small single-crystal InSb Hall sensor with an active volume approximately 35 μm wide by 110 μm long by 35 μm thick. The specifications and operation of this type of Hall sensor have been described previously.[10] A transport bridge about 230 μm wide and 5000 μm long was laser patterned into the YBCO film.

The Hall sensor was positioned over the film. The edge of the Hall sensor was approximately 35 μm from the side edge of the transport bridge with its long dimension along the bridge. Magnetic fields of up to 600 Oe were applied by a copper-wound magnet and applied parallel to the YBCO c axis and perpendicular to the plane of the bridge.

The local magnetic induction B_z was measured as a function of time on the transport bridge after a sequence of events that started with warming the bridge well above T_c. The bridge was then cooled in zero applied field and the temperature stabilized. The field was then cycled through half a hysteresis loop with the maximum applied field being large enough to place the superconductor in the remanent (trapped-flux) critical state. B_z was then measured as a function of time in this remanent state ($H_a=0$) and was typically monitored for 4000 seconds at a fixed temperature between 78 K and T_c. A transport current I_t was applied during the time interval 200 s $< t <$ 2000 s. This full sequence was repeated for each value of I_t. Since the Hall sensor was placed off-center, we can infer from symmetry considerations that application of a negative current is equivalent to having the Hall sensor moved to a position equidistant from the opposite side of the bridge during application of a positive current.

B_z measured at different values of applied transport current I_t are shown in Fig. 1. The results for I_t values of 0, $\pm$60, and $\pm$100 mA are presented. Several time segments have been defined in Fig. 1. The time $t=0$ is defined as the point at which the magnetic field returns to zero. The segment t_{ab} is the time between $t=0$ and the application of a transport current, segment t_{cd} is the time during which the current is applied, and segment t_{ef} is the time between turning off the current and the end of data acquisition. The results of Fig. 1 show the nearly logarithmic time decay typical of YBCO.[11] Prior to the application of a transport current, all the data have approximately the same logarithmic dependence, with a slight spread of initial B_z values resulting from small variations in the preparation of the critical state. As seen

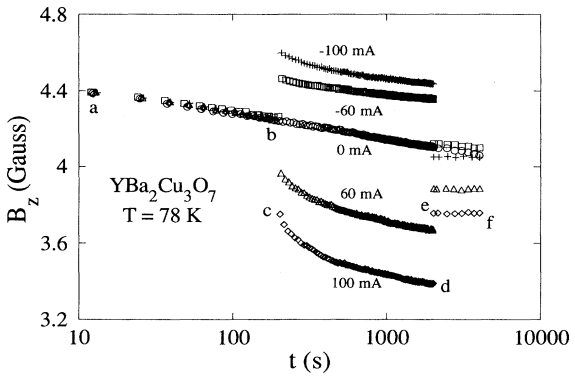

FIG. 1. Time dependence of the local magnetic induction B_z for different values of applied transport current in a YBCO film at $T=78$ K. In separate runs, either positive or negative currents were applied during the time segment between points c and d (t_{cd}). Current values of 0, $\pm$60, and $\pm$100 mA are presented. The critical current $I_c \approx 1.6$ A at $T=78$ K.

in Fig. 1, when a positive I_t is applied, there is a decrease in B_z, while for negative currents there is an increase in B_z. There is a clear asymmetry in the shape of the curves during t_{cd} which is associated primarily with relaxation processes. During t_{de} the curves have small values of the slope $dM/d\ln(t)$.

The critical current density J_c was determined by calibrating magnetic J_c measurements made over the temperature range from 78 to 90 K with transport J_c (current-voltage) measurements made from 87.5 to 90 K. At $T=78$ K a value $J_c \approx 2.2\times10^6$ A/cm^2 was determined.

In order to explain our results, we start by developing a general theoretical method for calculating hysteretic field and current distributions in a thin superconducting film whose thickness d is on the order of the penetration depth λ. We assume that the local vortex density $n(x)$ is related to the local transverse component of the magnetic flux density $B_z(x)$ via $B_z = n\phi_0$, where $\phi_0 = h/2e$ is the superconducting flux quantum. We ignore the spatial variation of the current density over the thickness of the film, and in this paper $J(x)$ refers to the current density averaged over the film thickness.

It has been shown that the normalized relaxation rate $S = (1/M_0)[dM\ln(t)]$ is nearly a constant for all YBCO materials.[12] Such relaxation can be seen in Fig. 1. However, here we model the case without relaxation. The volume of the film is divided into well-defined regions of two types. (a) Regions in which $|J(x)| = J_c$, where the current density is constant and the local field B_z may take on whatever value is determined by the current distribution and the applied field. (b) Regions in which $|J(x)| < J_c$, where the vortices are immobile and B_z is frozen at its previous value. The current distribution $J(x)$ therefore must adjust to keep B_z independent of time in this field-invariant region. Variations of the applied field or transport current displace the boundary location between these two regions.

The distribution of the transport current in a thin film of width $2W$ initially containing no vortices in the absence of an applied field was calculated analytically by Norris[13] as

$$\begin{aligned} &(2J_c/\pi)\tan^{-1}\{[(W^2-a^2)/(a^2-x^2)]^{1/2}\}, \quad -a<x<a\ , \\ &J(x)=J_c, \quad a\le x\le W\ , \end{aligned} \tag{1}$$

where $2a$ is the width of the vortex-free central region where $B_z=0$. Here we make use of the properties of Eq. (1) to show how it is possible to calculate the field and current distributions in a thin superconducting film in the presence of both an applied field and a transport current. To demonstrate our approach for a specific case, we first consider the influence of a transport current I_t upon the current and field distribution for a superconducting film initially in the remanent state; the starting field distribution is the trapped-flux critical state produced by applying a substantial applied field in the z direction and then reducing it to zero. The solid curve in Fig. 2(a) shows the initial current-density distribution, which has $J_y(x)=J_c$ for $0<x<W$ and $J_y(t)=-J_c$ for $-W<x<0$; the solid

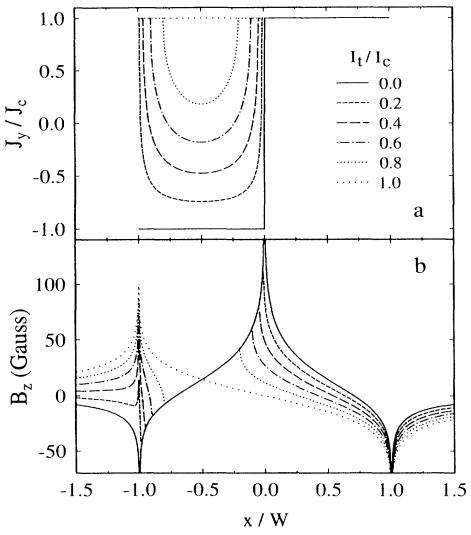

FIG. 2. (a) Calculated reduced current density J_y/J_c flowing in a thin film superconductor as a function of position x for different values of the transport current I_t applied in the y direction. (b) Calculated z component of the magnetic induction B_z at the film surface as a function of position x, for the same values of I_t. The center of the film is $x=0$, while the film edges are at $x/W=\pm 1$. B_z is calculated for a film with $J_c=2.2\times 10^6$ A/cm^2 at $T=78$ K. I_t is applied after establishing the remanent critical state in the film.

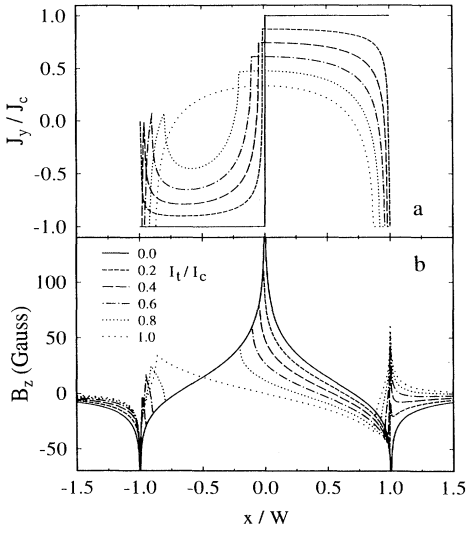

FIG. 3. Calculated distributions of (a) J_y/J_c and (b) B_z after applied transport current I_t is turned off. I_t was applied after establishing the remanent critical state in the film.

curve in Fig. 2(b) shows $B_z(x)$, the corresponding field distribution in the plane of the film.

The other curves in Figs. 2(a) and 2(b) show the distributions of $J_y(x)$ and $B_z(x)$ when a transport current I_t is applied in the y direction up to the maximum value $I_c=2WdJ_c$. Each curve of $J_y(x)$ is constructed by linear superposition of the remanent-state current-density distribution [solid lines in Fig. 2(a)] and a transport-current current-density distribution [obtained from Eq. (1)], which leaves $B_z(x)$ unchanged in the field-invariant region where $|J_y(x)|<J_c$. Two important modifications of Eq. (1), however, are needed to calculate $J_y(x)$ when the remanent state is perturbed by the application of I_t. The first is that the added transport current flows only in the region $-W<x<0$ symmetrically about the line $x=-W/2$, and the second is that the amplitude is twice as large as in Eq. (1), since the current density $J_y(x)$ just outside the frozen-flux region changes by $2J_c$ from $-J_c$ to $+J_c$. As I_t increases, the field-invariant region of width $2a$ shrinks, and the regions where $J=J_c$ expand until J_c is reached everywhere. Integration of Eq. (1) with the above modifications yields a nonlinear dependence of a upon I_t:

$$a=(W/2)[1-(I_t/I_c)^2]^{1/2} . \tag{2}$$

Next we consider the case for which the transport current is raised to some given value I_t and then reduced back to zero. The decrease of the current to zero is equivalent to the application of a negative current $(-I_t)$ relative to an initial state depicted by one of the curves in Fig. 2(a). The negative-current current-density distribution flows over the entire film volume according to Eq. (1), but with a double amplitude and a field-invariant region given by $a=W[1-(I_t/2I_c)^2]^{1/2}$.

The various curves in Fig. 3 show the final current and field distributions produced after a transport current has been applied in the y direction to the value I_t and then reduced to zero. An interesting case is that shown by the dotted curves in Fig. 3, for which $I_t=I_c$, which erases all memory of the remanent state. After the transport current has been reduced to zero, $J_y(x)=-J_c$ at the edges of the film and $|J_y(x)|<J_c$ in the field-invariant region of width $2a=W\sqrt{3}$, while the integral of $J_y(x)$ over the film width is zero.

We can now analyze the experimental data in Fig. 1 by comparing the results with the calculated field profiles in Figs. 2(b) and 3(b). The Hall sensor is centered at about $x_s=0.5W$ and would average the field over the sensor's width of about $0.3W$ if it were in the plane of the film. However, since the sensor is positioned about 30 μm above the film surface, it essentially senses an average field over a width on the order of W. Applying a negative I_t is equivalent to placing the sensor at $x_s=-0.5W$ in Figs. 2 and 3.

Increasing I_t decreases the average field at $x_s>0$ in Fig. 2(b) and increases to a lesser extent the average field at $x_s<0$. This is consistent with the positive and negative applied current results, respectively, shown in Fig, 1. After the current is turned off, the average field at $x_s<0$ is close to its original value, whereas at $x_s>0$ the average final B_z is reduced approximately linearly with I_t [Fig. 3(b)]. This type of behavior is indeed observed experimentally, as shown in Fig. 4 by the B_z value at $t=t_e$.

The theoretical results also provide us with some insight into the relaxation behavior in the presence of a transport current. The local relaxation rate depends on the driving force due to the interaction of the vortices with the local current density. Hence, at $x_s>0$ in Fig. 2,

even though B_z has dropped substantially, we expect the relaxation rate to remain at about its original value, since $J=J_c$. At $x_s<0$, on the contrary, B_z has not changed but $|J|$ has dropped significantly, and therefore one expects a strong reduction in the relaxation rate. This tendency is clearly visible in Fig. 1 at times close to t_d after the initial response to the abrupt current change has settled down.

After the transport current has been reduced back to zero, Fig. 3(a) shows that $|J|<J_c$ in almost all of the film's volume even for small I_t. This behavior is fundamentally different from that in slab geometry, where a small I_t leaves the current unchanged in most of the volume of the slab. We therefore expect the relaxation rate to drop rapidly with increasing I_t in the film geometry. Indeed, Fig. 4 shows a rapid drop in the relaxation with increasing I_t after current removal. The low relaxation rate is also directly visible in Fig. 1 for $t>t_e$.

In conclusion, we have measured the effect of an applied transport current on the local magnetic field of a YBCO thin film and presented theoretical calculations describing the corresponding development of the critical state in a thin film resulting from the transport current. The calculated behavior in a thin film is substantially different from that of the Bean critical state in a long slab in a parallel field. Starting from the remanent critical state, in the slab geometry $|J(x)|$ is equal to J_c, whereas in thin films a continuous distribution of current densities $J(x)$ is found. This feature results in a unique distribution of the magnetic field B_z and unusual magnetic relaxation behavior in the presence of a transport current. The approach outlined in this paper should make it possible to calculate ac flux-pinning losses arising from hysteretic magnetic flux penetration into type-II superconductors in many cases of practical interest. Two examples are (a) the high-power-level losses in thin-film strips used in high-temperature superconducting passive microwave devices and (b) the ac losses in flattened superconducting filaments in multifilamentary superconducting/normal (e.g., Bi-Sr-Ca-Cu-O/Ag) tapes.

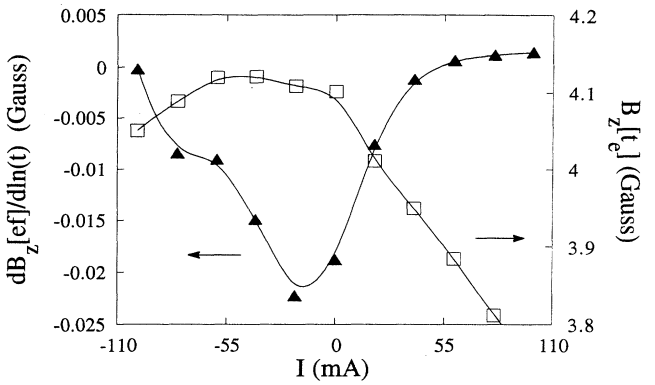

FIG. 4. Plotted are values of B_z at $t=t_e$ and the relaxation rate $dB_z(ef)/d\ln(t)$ both measured after turning off the transport current I_t. Both B_z and $dB_z(ef)/d\ln(t)$ are presented as functions of the transport current value I_t.

We would like to thank M. Konczykowski for the Hall sensors and useful discussions. The work at Purdue University and Ames Laboratory was supported in part by the Director for Energy Research, Office of Basic Energy Sciences. The work of Purdue University was supported by the Midwest Superconductivity Consortium (MISCON) through DOE Grant No. DE-FG02-90ER45427. Ames Laboratory is operated for the U.S. Department of Energy by Iowa State University under Contract No. W-7405-Eng-82. One of the authors (E.Z.) was supported by the Philip M. Klutznick fund and by the Israeli Ministry of Science Grant No. 5797. Another one of the authors (J.D.) was supported in part by the Purdue Research Foundation and another (M.I.) was supported in part by the Alexander von Humbolt Foundation.

*Permanent address: Institute of Solid State Physics, Russian Academy of Sciences, 142432 Chernoglovka, Russian Federation.

[1]C. P. Bean, Rev. Mod. Phys. **34**, 31 (1964).
[2]A. M. Campbell and J. E. Evetts, Adv. Phys. **21**, 199 (1972).
[3]M. A. R. LeBlanc, Phys. Rev. Lett. **11**, 149 (1963).
[4]K. Yasukochi, T. Ogasawara, N. Usui, and S. Ushio, J. Phys. Soc. Jpn. **19**, 1649 (1964).
[5]W. F. Druyvesteyn, Phys. Lett. **14**, 275 (1965).
[6]H. Theuss, A. Forkl, and H. Kronmüller, Physica C **190**, 403 (1992).
[7]L. D. Landau and E. M. Lifshitz, *Theoretical Physics, Vol. VIII: Electrodynamics of Continuous Media* (Pergamon, Oxford, 1963).
[8]V. L. Newhouse, *Applied Superconductivity* (Wiley, New York, 1964).
[9]R. P. Huebener, R. T. Kampwirth, and John R. Clem, J. Low Temp. Phys. **6**, 275 (1972).
[10]M. Konczykowski, F. Holtzberg, and P. Lejay, Superconduct. Sci. Tech. **4**, S331 (1991).
[11]J. R. Thompson, Yang Ren Sun, and F. Holtzberg, Phys. Rev. B **44**, 458 (1991).
[12]A. P. Malozemoff and M. P. A. Fisher, Phys. Rev. B **42**, 6784 (1990).
[13]W. T. Norris, J. Phys. D **3**, 489 (1970).